

Behaviour of a PEMFC supplying a low voltage static converter

I. Sadli*, P. Thounthong, J.-P. Martin, S. Raël, B. Davat

Institut National Polytechnique de Lorraine (INPL), GREEN-CNRS (UMR 7037), 2, Avenue de la Forêt de Haye, 54516 Vandœuvre-lès-Nancy, France

Available online 3 November 2005

Abstract

This paper presents the behaviour of a proton exchange membrane fuel cell (PEMFC) connected to a static dc–dc converter. Two different models of the PEM fuel cell are obtained from static measurements and impedance spectroscopy. The paper points out the necessity to use different models according to the type of study performed on the system. The comparison of models at high semiconductors switching frequency (25 kHz) is illustrated. Various experimental results obtained on a 500 W PEMFC test bench are compared with simulation ones to illustrate the accuracy of the proposed models.

© 2005 Elsevier B.V. All rights reserved.

Keywords: Proton exchange membrane fuel cell; Impedance spectroscopy; Static converter

1. Introduction

A proton exchange membrane fuel cell (PEMFC) is an electrochemical device that combines hydrogen fuel and oxygen to produce electricity, heat and water [1]. It has captured worldwide attention as a clean power source for various applications (electric vehicles, cogeneration, . . .).

In many applications of fuel cells, the treatment of the delivered energy is carried out by static converters. The integration of fuel cell in a power electronic environment (static converter–electric load) requires the knowledge of a model of the generator. This model allows studying the whole system as presented in Fig. 1, including fuel cell, converter, load and control.

Two models based on static characteristic and electrical impedance of a PEM fuel cell are presented and associated with the modeling of a dc–dc static converter. Then, the behaviour of the whole system is considered, first for low dynamic transient during load disturbance, and second at the static converter control frequency (25 kHz). Different experimental results are compared with simulation ones to illustrate the proposed modeling.

2. Fuel cell model

Two different models are considered. The first one is obtained for large variation of the load parameters. The fuel cell is represented by means of its voltage–current characteristic obtained in static operating mode [1]. The second one allows studying fuel cell voltage behaviour at the semiconductor switching. This simple model, obtained around an operating point, is defined by a voltage source and an electrical impedance.

2.1. Static model of PEM fuel cell

Fig. 2 presents the fuel cell voltage as a function of the current magnitude [1]. The obtained curve is composed of three main regions corresponding to the electrochemical activation phenomena (region 1), a linear part where the voltage drop is due to electronic and ionic internal resistances (region 2) and the last part where the diffusion kinetics of gases through the electrodes becomes the limiting factor (region 3). This last zone is characterized by a sharp voltage fall.

This voltage–current characteristic fuel cell compartment can be defined as follow [1]:

$$V_{FC} = E - A \ln \left(\frac{I_{FC} + i_n}{i_o} \right) - R_m(I_{FC} + i_n) + B \ln \left(1 - \frac{I_{FC} + i_n}{i_L} \right) \quad (1)$$

* Corresponding author. Tel.: +33 383 59 56 54; fax: +33 383 59 56 53.
E-mail address: Idris.Sadli@ensem.inpl-nancy.fr (I. Sadli).

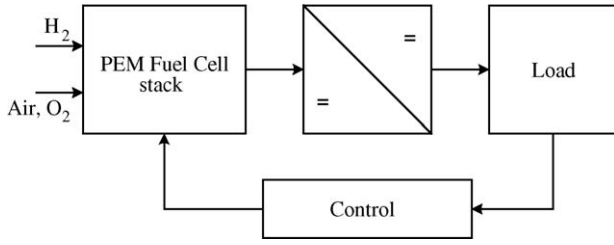


Fig. 1. Functional diagram of a fuel cell system.

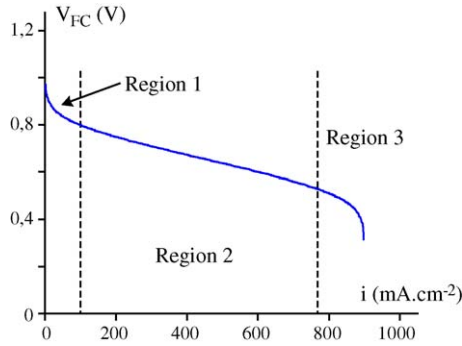


Fig. 2. Static fuel cell characteristic.

where E is the reversible no loss voltage of the fuel cell; I_{FC} the delivered current; i_0 the exchange current; A the slope of the Tafel line; i_L the limiting current; B the constant in the mass transfer term; i_n the internal current and R_m represents the membrane and contact resistances.

2.2. Impedance model of fuel cell

In the case of a PEM fuel cell, the electric energy is obtained by a redox electrochemical reaction [1]. The simplest small signal model for this type of reaction proposed by Randles can be used to modelize PEM fuel cell (Fig. 3). It contains a transfer resistance R_t , which characterizes the ions transfer phenomena at the electrodes (only cathode is represented), a resistance R_m representing the membrane and contact resistances, a double layer capacitor C_{dl} and a diffusion convection impedance $Z_{W\delta}$ expressed by Nernst for a finished diffusion length by the following relation [2,3]:

$$Z_{W\delta}(s) = R_d \frac{\text{th}(\sqrt{\tau_d s})}{\sqrt{\tau_d s}} \tag{2}$$

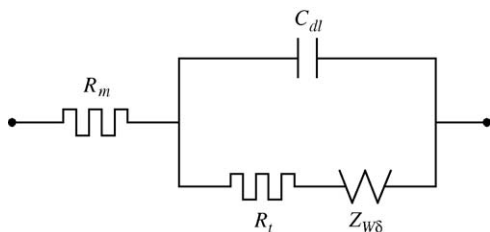


Fig. 3. Randles model.

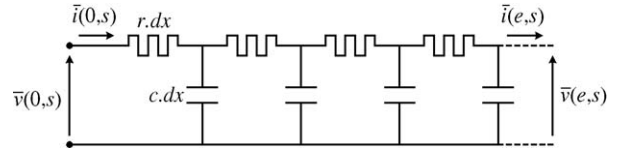


Fig. 4. Transmission line model.

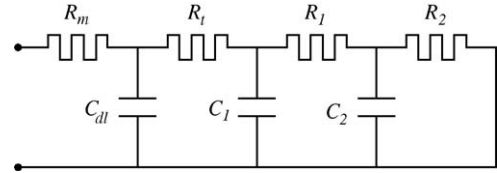


Fig. 5. Proposed model.

where R_d is the diffusion resistance, τ_d the diffusion constant time, and s is the Laplace operator.

In order to model this diffusion convection impedance by discrete elements, it can be first considered as a constants distributed transmission line (Fig. 4).

The input variables are linked to the output ones by:

$$\begin{bmatrix} \bar{v}(0, s) \\ \bar{i}(0, s) \end{bmatrix} = \begin{bmatrix} \text{ch}(me) & \frac{r}{m} \text{sh}(me) \\ \frac{m}{r} \text{sh}(me) & \text{ch}(me) \end{bmatrix} \cdot \begin{bmatrix} \bar{v}(e, s) \\ \bar{i}(e, s) \end{bmatrix} \tag{3}$$

with $m = \sqrt{rcs}$, and where e is the line length.

If the line is short circuited at its end ($x=e$), its impedance becomes:

$$Z_1(s) = R \frac{\text{th}(\sqrt{RCs})}{\sqrt{RCs}} \tag{4}$$

where R and C are the total line resistance and capacitance ($R = re$ and $C = ce$).

This impedance has the same form that the one given in relation (2). Then one can represent the diffusion convection impedance by such a model with a finite number of branches. The

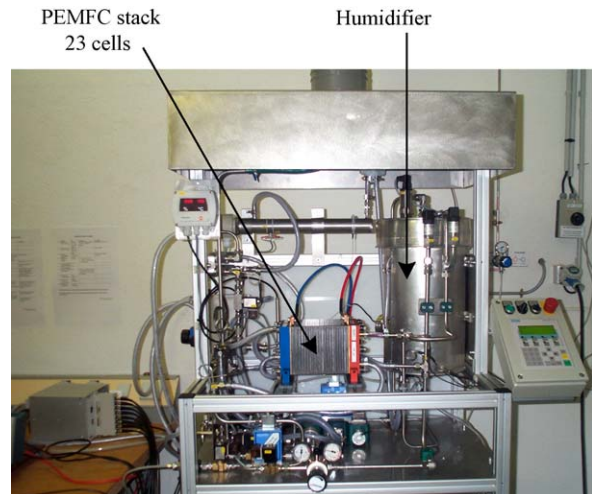


Fig. 6. ZSW (Ulm, Germany) 500 W PEMFC test bench.

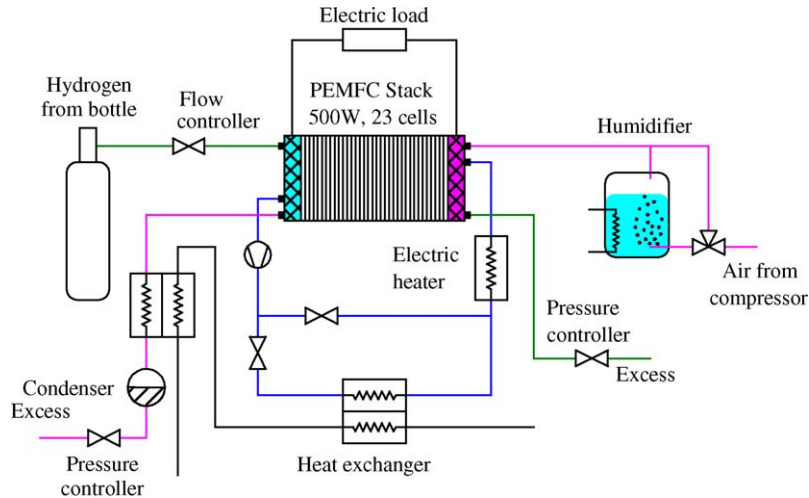


Fig. 7. Simplified diagram of the 500 W PEM fuel cell system.

simplest model proposed is represented in Fig. 5 and contains for this impedance two different branches, R_1-C_1 and R_2-C_2 .

3. Test bench presentation

The test bench, presented in Fig. 6 and schemed in Fig. 7, uses a 500 W PEMFC stack. Air is supplied from a compressor through a humidification unit, and pure dry hydrogen comes from bottles. A cooling system permits to impose a constant stack temperature by heating or cooling the water circuit. A programmable control unit contains all necessary control functions, such as reference setting, measurement conditioning and security shutdown. The stack contains 23 cells with an active surface of 100 cm^2 [6].

The experimentation is carried out under a stack temperature of 55°C , a humidifier temperature of 45°C , and a use of hydrogen and air, respectively, of 50 and 25% at atmospheric pressure.

4. Fuel cell model identification

4.1. Static characteristic of the fuel cell

Experimental identification of parameters of relation (1) leads to: $E = -\Delta G/2F = 27.1\text{ V}$ (for $T = 55^\circ\text{C}$ and 23 cells), $A = 1.35\text{ V}$, $i_o = 6.54\text{ mA}$, $R_m = 42\text{ m}\Omega$, $B = 1.19\text{ V}$, $i_L = 100\text{ A}$ and $i_n = 230\text{ mA}$. Fig. 8 compares the experimental stack voltage with the calculated ones deduced from these parameters.

4.2. Impedance model of the fuel cell

Thanks to the impedance spectroscopy method on a large range of frequency [2–5] and a least square method identification, the parameters of the model of Fig. 5 can be obtained.

For the considered PEMFC, one obtains $R_m = 42\text{ m}\Omega$, $R_t = 38\text{ m}\Omega$, $C_{dl} = 19\text{ mF}$, $R_1 = 40\text{ m}\Omega$, $R_2 = 22\text{ m}\Omega$, $C_1 = 0.15\text{ F}$, $C_2 = 2.37\text{ F}$. Fig. 9 presents the measured and calculated impedances by the proposed model (Fig. 5) for rated current (40 A).

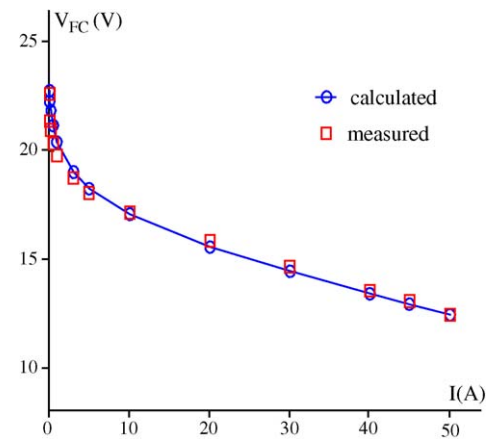


Fig. 8. Static characteristic of the 500 W PEMFC (calculated point obtained from relation (1)).

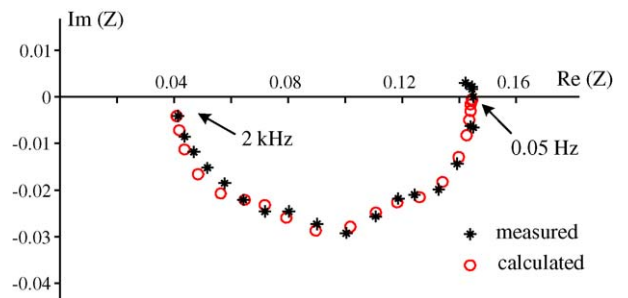


Fig. 9. Measured and calculated impedance for the rated current of 40 A and a frequency range of 0.05–2000 Hz.

5. Fuel cell converter

5.1. Converter operation

To adapt the low dc voltage delivered by the fuel cell to a standard 42 V automotive dc bus, a boost converter – operating in continuous mode – is used, as shown in Fig. 10. This converter is composed of a high frequency inductor L , an output filtering capacitor C , a diode D_1 and a main switch S_1 . Switch S_2 is a

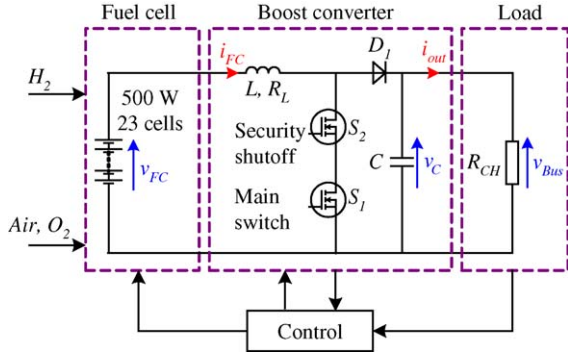


Fig. 10. Boost converter.

shutdown device to prevent the fuel cell stack from short circuit in case of accidental destruction of S_1 , or of faulty operation of the regulator.

5.2. Power circuit design

The design of the converter is detailed in [7]. With a 12.5 V–40 A fuel cell and assuming an efficiency of 90% for the converter with a switching frequency of 25 kHz, a bus voltage ripple of 2% and an input current ripple of 12% of the rated value one obtains:

$$\begin{aligned} P_{\text{out}} &= 450 \text{ W}, & I_{\text{out}} &= 10.7 \text{ A}, & I_{C,\text{rms}} &= 19.1 \text{ A}, \\ L &= 72.9 \mu\text{H}, & I_{S,\text{rms}} &= 33.5 \text{ A}, & I_{D1,\text{rms}} &= 21.9 \text{ A}, \\ C &= 357 \mu\text{F} \end{aligned} \quad (5)$$

Note that three capacitors C (10 mF, 100 V, 7.32 A) are selected, associated in parallel to respect the constraint on RMS capacitor current. The whole input capacitance is therefore 30 mF, so that voltage ripple is much lower than 2%.

5.3. FC converter modeling

5.3.1. Switching model

In order to design controller and to develop system simulation, the switching model of fuel cell converter has to be known [8]. The non-linearity due to the power semiconductor devices is negligible, but parasitic resistances of the power semiconductor devices, inductor and capacitor are considered. The load of the converter is classically modeled by a resistance R_{CH} . The operating state of the boost converter is represented by the a state vector $X(t)$ which contains the fuel cell current $i_{FC}(t)$ and the capacitor voltage $v_C(t)$:

$$X(t) = \begin{bmatrix} i_{FC}(t) \\ v_C(t) \end{bmatrix}$$

When S_1 is on, state differential system is:

$$\begin{cases} \frac{d}{dt} X(t) = A_1 X(t) + U_1(t) \\ v_{\text{Bus}} = C_1 X(t) \end{cases} \quad (6)$$

with:

$$A_1 = \begin{bmatrix} -\left(\frac{R_L + R_M}{L}\right) & 0 \\ 0 & -\frac{1}{C} \left(\frac{1}{R_{CH} + R_C}\right) \end{bmatrix},$$

$$U_1(t) = \begin{bmatrix} \frac{v_{FC}(t)}{L} \\ 0 \end{bmatrix}, \quad C_1 = \begin{bmatrix} 0 & \frac{R_{CH}}{R_{CH} + R_C} \end{bmatrix}.$$

When S_1 is off, state differential system is:

$$\begin{cases} \frac{d}{dt} X(t) = A_2 X(t) + U_2(t) \\ v_{\text{Bus}}(t) = C_2 X(t) \end{cases} \quad (7)$$

with:

$$A_2 = \begin{bmatrix} -\frac{1}{L} \left(R_L + \frac{R_{CH} R_C}{R_{CH} + R_C} \right) & -\frac{1}{L} \left(\frac{R_{CH}}{R_{CH} + R_C} \right) \\ \frac{1}{C} \left(\frac{R_{CH}}{R_{CH} + R_C} \right) & -\frac{1}{C} \left(\frac{1}{R_{CH} + R_C} \right) \end{bmatrix},$$

$$U_2(t) = \begin{bmatrix} \frac{v_{FC}(t) - V_D}{L} \\ 0 \end{bmatrix},$$

$$C_2 = \begin{bmatrix} \frac{R_{CH} R_C}{R_{CH} + R_C} & \frac{R_{CH}}{R_{CH} + R_C} \end{bmatrix}$$

R_C is the equivalent series resistance (ESR) of the output capacitor, R_L the series resistance of the input inductor, R_M the whole drain–source on resistance MOSFETS, V_D the forward voltage drop of diode D_1 and $v_{FC}(t)$ is the fuel cell voltage.

5.3.2. Control structure

The control structure of the fuel cell converter designed with a classical cascade control is shown in Fig. 11.

To obtain the transfer function of the converter, the linearized differential equations from relations (6) and (7) are defined as follow [9,10]:

$$\begin{cases} L \frac{d\tilde{i}_{FC}(t)}{dt} = \tilde{v}_{FC}(t) - R_L \tilde{i}_{FC}(t) - (1 - D) \tilde{v}_{\text{Bus}}(t) + V_{\text{Bus}} \tilde{d}(t) \\ C \frac{d\tilde{v}_{\text{Bus}}(t)}{dt} = (1 - D) \tilde{i}_{FC}(t) - I_{FC} \tilde{d}(t) - \frac{\tilde{v}_{\text{Bus}}(t)}{R_{CH}} \end{cases} \quad (8)$$

where D is the nominal duty cycle of the PWM fuel cell converter, \tilde{d} the duty cycle variation, V_{Bus} the nominal dc bus voltage, \tilde{v}_{Bus} the dc bus voltage variation, I_{FC} the nominal fuel cell current, \tilde{i}_{FC} the fuel cell current variation, R_{CH} the load resistance and R_L is the series resistance of inductor L .

Note that series resistance of capacitor (R_C) and of the power semiconductor devices (R_M) are ignored. From Eq. (8), the fuel cell current loop can be modeled by the following open loop transfer function:

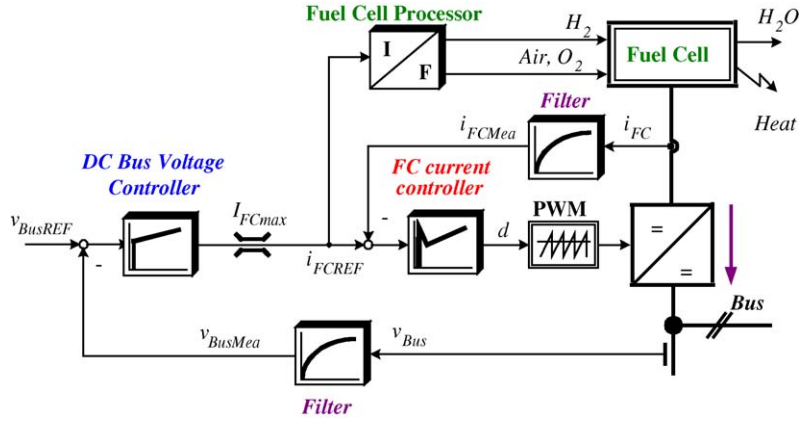


Fig. 11. Cascade voltage and average-current control structure of the PEMFC converter.

$$\left. \frac{I_{FCMea}(s)}{I_{FCREF}(s)} \right|_{OL} = \underbrace{G_{Ci} \frac{(T_{Ci}s + 1)(T_{Cd}s + 1)}{T_{Ci}s}}_{\text{Current controller}} \underbrace{\frac{1}{V_P}}_{\text{PWM}} \times \underbrace{\frac{I_{FC}(s)/d(s)}{\left(\frac{s}{\omega_n}\right)^2 + \frac{2\zeta}{\omega_n}s + 1}}_{\text{Current filter}} \underbrace{\frac{K_1}{T_{fc}s + 1}}_{\text{Current filter}} \quad (9)$$

where V_P is the amplitude of the PWM saw tooth carrier signal, K_1 the gain of measured fuel cell current, T_{fc} is the current filter time constant and:

$$G_I = \frac{(1 - D)R_{CH}I_{FC} + V_{Bus}}{R_L + R_{CH}(1 - D)^2},$$

$$T_z = \frac{V_{Bus}R_{CH}C}{(1 - D)R_{CH}I_{FC} + V_{Bus}},$$

$$\omega_n = \sqrt{\frac{R_L + R_{CH}(1 - D)^2}{LCR_{CH}}},$$

$$\zeta = \frac{1}{2} \frac{L + R_L R_{CH}C}{R_L + R_{CH}(1 - D)^2} \omega_n \quad (10)$$

An analogical PID controller is selected for fuel cell current controller. The derivation time constant T_{Cd} is chosen in order to compensate the filter pole $-1/T_{fc}$. By classical controller design, the gain G_{Ci} and the integration time constant T_{Ci} are set to obtain a defined phase margin (about 55°).

As far as the dc bus voltage loop is much slower than the fuel cell current loop, the open loop transfer function between dc bus voltage measure and dc bus voltage reference can be written as:

$$\left. \frac{V_{BusMea}(s)}{V_{BusREF}(s)} \right|_{OL} = \underbrace{G_{CV} \frac{(T_{CV}s + 1)}{T_{CV}s}}_{\text{Voltage Controller}} \underbrace{\frac{1}{K_1}}_{\text{Current Loop}} \times \underbrace{\frac{V_{Bus}(s)/I_{FC}(s)}{G_V(1 - T_{Zv}s)}}_{\text{Voltage filter}} \underbrace{\frac{K_2}{T_{fv}s + 1}}_{\text{Voltage filter}} \quad (11)$$

where K_2 is the gain of the measured dc bus voltage, T_{fv} is the voltage filter time constant and:

$$G_V = \frac{R_{CH}(V_{Bus}(1 - D) - I_{FC}R_L)}{(1 - D)R_{CH}I_{FC} + V_{Bus}},$$

$$T_{Zv} = \frac{LI_{FC}}{V_{Bus}(1 - D) - I_{FC}R_L},$$

$$T_v = \frac{V_{Bus}R_{CH}C}{(1 - D)R_{CH}I_{FC} + V_{Bus}} \quad (12)$$

A PI controller is selected for dc bus voltage controller, and the gain G_{CV} and the integration time constant T_{CV} are set to obtain a defined phase margin (about 55°), as well.

6. Fuel cell with static converter

6.1. Load variation

In order to confirm fuel cell converter operation and to compare experimental results and simulation ones, one has represented in Figs. 12 and 13 the system response to a load step. The model used for the PEMFC is the static ones detailed in relation (1). Fig. 13 shows the experiment behaviour of the fuel

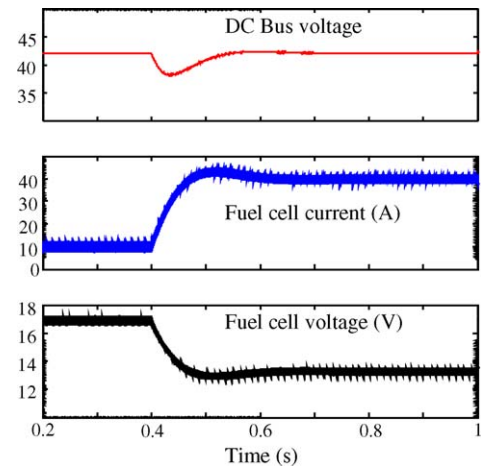


Fig. 12. Simulation PEMFC converter response with load disturbance.

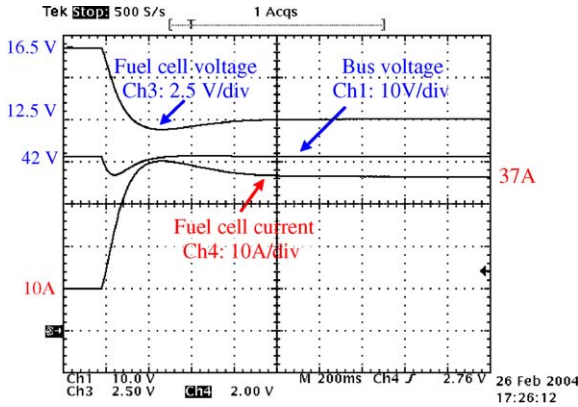


Fig. 13. Experimental PEMFC converter response with load disturbance.

cell voltage response for a load step, this response is almost of resistive nature. The voltage drop corresponds to low frequency resistance, which is identified in Fig. 9 at 5 mHz. The physical significance of this resistance is due to the sum of a membrane, mass transfer resistance and diffusion phenomena.

6.2. High frequency behaviour

Figs. 14 and 15 show simulation and experiment on fuel cell current and voltage at 25 kHz, the switching frequency of the boost converter, and rated power (40 A, 12.5 V).

The simulation and experimental results follow the same behaviour. The static model, which uses a dc resistance, leads for a given duty cycle to a bigger voltage ripple for the fuel cell voltage. The ripples obtained with the dynamic model are closed to the ones deduced from the experimental results: 4.7 A against 4.2 A for the fuel cell current, and 211 mV against 185 mV for the fuel cell voltage. These differences are not so important if one considers that one has taken into account the fuel cell model, and the parasitic resistances of the boost converter. The relationship between the ripple magnitude of fuel cell voltage and current gives exactly the value of the membrane and contact resistance. This value is identified in Fig. 9, is the real part of the

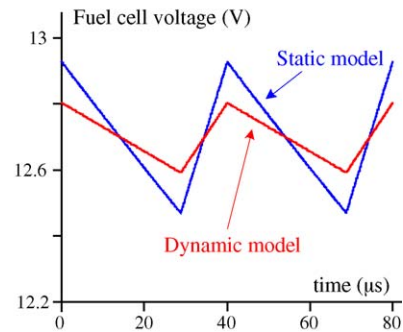
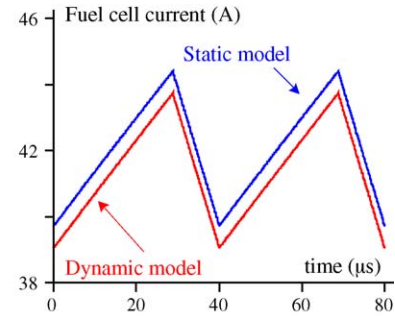
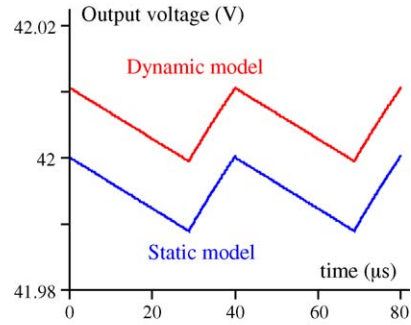


Fig. 15. Simulation results at 40 A.

high frequency (2 kHz) measured impedance, and is estimated at 42 mΩ.

7. Conclusion

The main objective of this work is to use different models in the simulation of a proton exchange membrane fuel cell with dc–dc converter. The experimental and simulated results obtained with a 500 W PEM fuel cell are closed to the ones deduced from simulation as well as for the static model used in low dynamic load transient than for the dynamic model at the converter switching frequency. Experimental results at high frequency switching of the semiconductor, show that fuel cell electrical behaviour is mostly resistive, associated to membrane resistance, which is accurately described by the dynamic model.

References

[1] J. Larminie, A. Dicks, Fuel Cell Systems Explained, second ed., John Wiley & Sons, 2003.
 [2] J-P. Diard, B. Gorrec, C. Montella, Cinétique Electrochimique, Hermann, 1996.

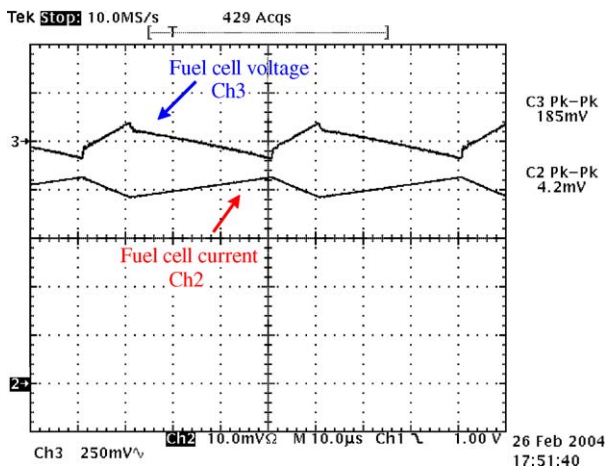


Fig. 14. Experimental FC voltage and current at 40 A.

- [3] J.R. Macdonald, *Impedance Spectroscopy*, Wiley, 1987.
- [4] T.E. Springer, I.D. Raistrick, J. Electrochem. Soc. 136 (1998) 1594–1603.
- [5] J.-P. Diard, B. Le Gorrec, C. Montella, C. Poinignon, G. Vitter, J. Power Sources 74 (1998) 244–245.
- [6] W. Friede, S. Raël, B. Davat, IEEE Trans. Power Electron. 19 (2004) 1234–1241.
- [7] P. Thounthong, S. Raël, B. Davat, Test of a PEM fuel cell with low voltage static converter. J. Power Sources (2005), in press, available from: <http://authors.elsevier.com/sd/article/S0378775305001564>.
- [8] E.V. Dijk, H.J.N. Spruijt, D.M. O’Sullivan, J.B. Klaassens, IEEE Trans. Power Electron. 10 (1995) 659–665.
- [9] R.D. Middlebrook, S. Cuk, Int. J. Electron. 42 (1977) 521–550.
- [10] V. Vorperian, IEEE Trans. Aerospace Electron. Syst. 26 (1990) 490–496.